IRON LOSS COMPUTATION OF A PERMANENT MAGNET MOTOR: FEA-BASED COMPARATIVE STUDY BETWEEN DIFFERENT MODELS

H. MEL   A. MANSOURI

CES Laboratory, National Engineering School of Sfax, Soukra Street Km 3.5-BP W Sfax, Sfax, 3038, Tunisia,
hajermel@gmail.com
ali.mansouri@isetgf.rnu.tn

H. TRABELSI

CES Laboratory, National Engineering School of Sfax, Soukra Street Km 3.5-BP W Sfax, Sfax, 3038, Tunisia,
hafedh.trabelsi@enis.rnu.tn

Abstract: This paper aims to investigate iron losses in a surface mounted permanent magnet motor. For this, an overview of common iron loss models has been initially presented. Then, three different loss models have been applied for the computation of iron losses in the studied machine. The reason of testing several loss models is to discuss their advantages and disadvantages and to discuss their applicability, stability and efficiency. To perform this study, finite element method is used. Indeed, a considerable attention has been paid to the dynamic modeling of the rotating machine. Afterward, the employed models have been incorporated into the finite element analysis. Finally, the obtained results are compared and analyzed. Based on the obtained results, on one hand, it is revealed that traditional technique is fast and stable while the hysteresis models necessitates a lot of time and requires an adequate iterative procedure. On the other hand, it is shown that traditional technique is simplistic unlike the hysteresis models which are more general and accurate.

Key words: Iron losses, Synchronous permanent magnet motor, Iron loss models, Traditional technique, Preisach model, Hybrid technique, Transient finite element analysis.

1. Introduction

Nowadays, permanent magnet synchronous machines (PMSM) are currently used in a board range in electric vehicle applications [1] thanks to their remarkable advantages such as flexibility of control, higher torque capability, higher power density, higher efficiency [2-4]. Particularly, surface mounted permanent magnet synchronous machines have been extensively utilized owing to their compact structure, low weight and small size [5]. In this work, the considered topology is a surface mounted permanent magnet motor.

From a technique point of view, permanent magnet synchronous machines are basically made of ferromagnetic materials. That is why; these materials have been increasingly utilized. In fact, considerable attention has been paid to the investigation of ferromagnetic materials properties in order to improve machines performances and efficiency as well. For this, several ways have been studied. The most crucial way is the analysis of iron losses in these parts in order to be considered in the design procedure.

During recent years, the investigation of iron losses has been regarded as crucial issue. This fact has been considered an important subject of research. So, many works have been performed to deal with this problem [6-9]. Although the great amount of research that is done into that field, it has remained a challenge task up this date.

Generally, loss models may be classified under two main groups. The first group corresponds to models that estimate losses by post processing the magnetic field solution. Hence, losses are not included into the magnetic field solution. The second group represents models that integrate losses into the magnetic field solution.

In practice, it is difficult to deal with iron losses in a rotating electrical machine because of the complexity of the geometry and the interdependency of different physical phenomena that occur. In various zones of the magnetic circuit, the flux distribution is not pulsating with time in one direction. It is generally fully two-dimensional and highly distorted. Accordingly, efficient approach is required for accurate calculation of iron losses. In actuality, many researches have been performed to deal with this avoided.

This work aims for the computation of iron losses in a synchronous permanent magnet motor using three different techniques. For this end, an overview of iron loss models is presented. The studied machine is modeled by means of finite element method. Then, the adopted approaches are coupled with a two dimensional transient finite element analysis (FEA). So, many deep simulations are performed. Finally, the obtained results are discussed in order to show where these models fail and where they prevail and to discuss their effectiveness and their applicability.

2. Overview of Iron loss models

Fundamentally, the analysis of iron losses is a vital issue since it detriment electrical devices. To deal with this issue, many models have been developed in the literature. In the following, the most important and common models for iron losses are reviewed.

2.1 Traditional models

Historically, models used for the prediction of iron losses in ferromagnetic materials goes back to the well

known formula which is introduced by Steinmetz in 1892. Based on this approach, the lamination ferromagnetic material is supposed to be supplied by a unidirectional and sinusoidal magnetic flux. The iron losses are evaluated as follows [10]:

$$P = kf^{\alpha}B_m^{\beta}$$

(1)

Where

f is the frequency.

B_m is the peak value of the magnetic induction.

k, α and β are the model coefficients, depending on the used material.

After that, Steinmetz separated the total iron losses into hysteresis losses and eddy-current ones. Those losses are then expressed as follows [11]:

$$P = C_{hyst}fB_m^2 + C_{cl}f^2B_m^2$$

(2)

Where

C_{hyst} is the hysteresis loss coefficient

C_{cl} is the eddy current loss coefficient.

Afterwards, the original formula has undergone numerous modifications in order to be ameliorated. In 1988, Bertotti separated the total iron losses into hysteresis losses, eddy-current losses and excess losses. This loss theory states that under sinusoidal magnetization, the total iron losses are given by [12]:

$$P = P_{hyst} + \frac{\sigma d^2 \pi^2 B_m^2}{6}f + C_{exc}f^{1.5}B_m^{1.5}$$

(3)

Where

P_{hyst} represents the hysteresis losses

C_{exc} is the excess losses coefficient.

σ is d the conductivity of the used material

d is the lamination thickness.

Subsequently, this approach has become widely adopted by many researchers.

The previously presented iron loss models are generally based on the assumption of sinusoidally alternating magnetic flux. However, the magnetic flux in rotating machines is not unidirectional and sinusoidal; it is generally non sinusoidal and highly distorted. Fundamentally, the sources of the flux distortion are the slotting effects and the harmonics caused by pulse-width modulated (PWM) inverter... Consequently, the previous models have been undergone several modifications in order to account for arbitrary flux density waveforms and to improve the considered approximations.

Practically, the two-component method was modified to consider arbitrary flux waveforms and minor loops [13, 14]. In addition, in [15] the statistical loss theory of Bertotti has been generalized in order to consider the dependence of the eddy-current and excess losses on the magnetic flux density derivative. Accordingly, the iron losses are computed as follows:

$$P = P_{hyst} + \frac{\sigma d^2}{12}\int_0^T\left(\frac{dB}{dt}\right)^2 dt + C_{exc}\int_0^T\left|\frac{dB}{dt}\right|^{3/2} dt$$

(4)

Basically, the statistical loss theory of Bertotti is commonly used for the computation of iron losses under alternating field excitation and under rotational flux density waveform as well, by introducing some correcting factors for the hysteresis loss [16-18].

Recently, traditional approaches have been widely applied in research although they are generally considered grossly simplistic. The impetus for their attractiveness is thanks to the following reasons [19]: First, the implementation of those models is stable since only a lossless single-valued magnetization curve is required. In reality, the losses are calculated by post processing the magnetic field solution. Second, the identification of models parameters is simple. Third, the accuracy of the obtained results is acceptable in particular regimes and frequencies. Alternatively, the post processing models have many drawbacks which outweigh the aforementioned advantages. In fact, the extensions of the statistical theory of Bertotti are suitable only for applications performed in low frequency. In addition, the minor loops effects are not modeled properly. Furthermore, the effects of core losses on the machine characteristics cannot be examined.

2.2 Advanced techniques

Fundamentally, the track of the B-H behavior is so important for the prediction of magnetic losses because iron losses can be determined from the loops area. So, many models have been proposed in the literature to represent the relation ship between the magnetic flux density and the magnetic field intensity. Most of the developed models are summarized in the next paragraphs.

Physically, the magnetization process is complicated because of the numerous intrinsic complex phenomena that can occur during the magnetization mechanism. Those magnetic features are domain walls dynamics, hysteresis, and eddy current. Indeed, the hysteretic behavior is the most complex property of magnetic materials. Mainly, the modeling of this phenomenon is a crucial issue.

Generally, the term hysteresis is used to examine

rate-independent hysteresis. So, hysteresis loops are modeled purely. In fact, the investigation of the static hysteresis property only is considered basic and more comprehensible. However, from a physic point of view, eddy-current problem is an inherent property of ferromagnetic materials. These magnetic aspects are small details. So, it is difficult to deal with them.

Naturally, the hysteretic behavior and eddy-current effects are also physically interconnected. Therefore, it is vital to adequately model them. In that case, modeling hysteresis loops efficiently requires rate-dependent-hysteresis models. The rate of the magnetic field modifies the form of the hysteresis loop and enlarges its area; hence, it modifies the energy profile. On the basis of this study, dynamic loops shape has to be carefully modeled in order to assure accurate prediction of iron losses. For this end, advanced techniques have been proposed in the literature. In fact, many hysteresis models have been widely studied in the literature [20-22]. Most of them are static in nature. But, some of these approaches have been generalized in order to consider the dynamic effects. These techniques are physically based. They aim for the study of certain physic phenomena such as hysteresis by modeling the hysteresis loop shapes. Moreover, these models attempt to model iron losses properly by integrating losses in the magnetic field solution.

Below, the most important and common used models for hysteresis modeling are reviewed.

2.2.1 Static hysteresis models

The most popular static hysteresis models are Preisach model and Jiles-Atherton model. In deed, the static Preisach model was introduced by Frederick Preisach Neel in 1935 to describe the hysteresis loss [20]. It was considered a great invention because it is physically based. This approach assumes that magnetic material behavior can be descried via an infinite set of elementary rectangular hysteresis loops $\gamma_{\alpha\beta}(H)$. On the basis of Preisach theory, the flux density can be expressed as [21]:

$$B = \iint_S p(\alpha,\beta)\gamma_{\alpha\beta}(H)d\alpha d\beta$$

(5)

Where

α is the upper switching fields.

β is the lower

$p(\alpha,\beta)$ is the distribution function over the Preisach triangle in the Preisach plane.

S is the Preisach triangle that is mathematically defined as:

$$S = \{(\alpha,\beta) \mid \alpha \geq \beta, \beta \geq -H_s, \alpha \leq H_s\}$$

(6)

Where

H_s is the magnetic field intensity in the saturation.

Jiles-Atherton model was introduced by Jiles and Atherton in (1984, 1986) [22]. It is based on some hypothesis concerning the domain wall movement. The considered assumptions lead to a differential equation with five parameters to identify.

In [23, 24], it is stated that the Jiles-Atherton model is characterized by simplicity and speed. However, the implementation of this model requires many experimental data which are not usually available. It is also shown in the same articles that the attractive features of Preisach model are accuracy, efficiency and generality. These considerable advantages lead to its popularity.

2.2.2 Dynamic hysteresis models

Different methods have been proposed in the literature to model the dynamic hysteresis loops [25-28]. The most known models are the Preisach model, the Jiles-Atherton model and the E&S one. In this section, a brief review of the dynamic hysteresis models is provided.

In 1988, Mayergoyez tried to generalize the static property of the classic Preisach model to account for dynamic effects [24]. He constrained the distribution function to be dependent on the time derivative of the magnetic field. Therefore, the dynamic Preisach model is mathematically represented as follows [25]:

$$B = \iint_S p(\alpha,\beta,\frac{dB}{dt})\gamma_{\alpha\beta}(H)d\alpha d\beta$$

(7)

In 1992, Bertotti proposed a dynamic generalization of the Preisach hysteresis model [26]. This theory supposed that the Preisach operator switches at a finite rate to consider the dynamic effect. Similarly, Jiles has attempted to compel several modifications to the original model in order to take dynamic effects into account [27]. Furthermore, the Generalized Chua-type model has undergone several modifications to consider eddy-current effects. Then, the relationship between the magnetic field density and the magnetic field intensity is as follows [28]:

$$H = v^r B_1 + v^i \frac{\partial B_1}{\partial \tau} + \frac{\sigma w_1 d^2}{12} \frac{\partial B}{\partial \tau} \tau$$

(8)

Where

v^r is the reflectivity coefficient

v^i is the hysteresis one.

B_1 is the fundamental component of the magnetic induction

w_1 the fundamental component of the *.

τ Stands for

The lack of reliable experimental data hinders the use of these dynamic hysteresis models.

Advanced techniques aims for the investigation of iron losses more adequately seeing that they are physically based. Hence, they deal with some complicated phenomena. For instance, hysteresis loops including minor loops are properly modeled. Furthermore, according to these models iron losses are incorporated into the finite element analysis. So, they influence the field solution. Subsequently, the machine characteristics can be examined. Despite the above advantages, advanced models suffer from a remarkable problem which is high computation time. The convergence is also vulnerably reached in several cases.

2.3 Hybrid techniques

A technique which is referred to as hybrid technique is a combination between a hysteresis model and a post processing one. Hybrid techniques aim principally for the consideration of the majority of loss phenomena using simple concepts. According to these techniques, iron losses are generated and calculated from the total applied magnetic field strength which is decomposed in three components as follows [19]:

$$H(t,B) = H_h(t,B) + H_{cl}(t,B) + H_{ex}(t,B) \qquad (9)$$

Where

$H_h(t,B)$ represents the hysteresis component which is determined by employing a suitable static hysteresis model.

$H_{cl}(t,B)$ corresponds to the eddy-current component.

$H_{ex}(t,B)$ represents the excess component.

This approach is referred to as an hybrid techniques. Indeed it is a combination between a static hysteresis approach and an empirical one. Hybrid techniques are characterized by the generality, the stability and the ability to integrate the losses on the field solution.

3. Adopted models formulations

In this work, three different techniques have been adopted for the analysis of iron losses in the studied machine: a traditional technique, an advanced technique and a hybrid one.

Concerning the first method, the post processing model developed in [6] is employed for the estimation of iron losses in the studied topology. According to this model, iron losses are segregated into three components including hysteresis losses, eddy current losses and excess one. Then, they are computed using the following formulations [7]:

$$P(t) = P_{hyst}(t) + P_{cl}(t) + P_{ex}(t) \qquad (10)$$

$$P_{hyst}(t) = \left(\left| H_x \frac{dB_x}{dt} \right|^{\frac{2}{\beta}} + \left| H_y \frac{dB_y}{dt} \right|^{\frac{2}{\beta}} \right)^{\frac{\beta}{2}} \qquad (11)$$

$$P_{cl}(t) = K_c \left(\left(\frac{dB_x}{dt} \right)^2 + \left(\frac{dB_y}{dt} \right)^2 \right)$$

(12)
$$P_{ex}(t) = \frac{K_e}{C_e} \left(\left(\frac{dB_x}{dt} \right)^2 + \left(\frac{dB_y}{dt} \right)^2 \right)^{\frac{3}{4}}$$

(13)

Where

H_x is the radial components of the magnetic field intensity

H_y is the tangential component of the magnetic field intensity

B_x is the radial component of the induction

B_y is the tangential component of the induction.

β, K_c, K_e and C_e are the model parameters.

The model parameters are determined using experimental data.

If the magnetic field varies with a periodic manner, the average iron loss density can be determined by integrating the previous equations over half period as follows:

$$P_{hyst} = \frac{2}{T} \int_T P_{hyst}(t) dt \qquad (14)$$

$$P_{cl} = \frac{2}{T} \int_T P_{cl}(t) dt \qquad (15)$$

$$P_{ex} = \frac{2}{T} \int_T P_{ex}(t) dt \qquad (16)$$

Where

T is the period.

Since this model is incorporated into two dimensional finite element analyses, the hysteresis losses can be obtained by summing hysteresis losses per element over the elements number. Then, the total hysteresis losses are obtained as follows:

$$P_{h,st} = 2pfL$$

$$\sum_{i=1}^{Ne} A_{ei} \left(\sum_{j=1}^{N} \left(\left| H_{ex,t_j}(B_{ex,t_j} - B_{ex,t_{j-1}}) \right|^{\frac{2}{\beta}} + \left| H_{ey,t_j}(B_{ey,t_j} - B_{ey,t_{j-1}}) \right|^{\frac{2}{\beta}} \right)^{\frac{\beta}{2}} \right) \quad (17)$$

The used magnetic parameters are determined for each finite element e at any time step t_j.

Where

p is the pair pole number,

L is the machine length,

A_{ei} is the area of the element number i,

N_e is the total number of elements mesh

N is the total number of finite element analysis steps.

The above equation has been coupled with the finite element analysis in order to determine the iron losses in the studied motor.

Similarly, the classical eddy current loss is determined as:

$$P_{cl} = 8.p.K_c N.f^2.L.$$

$$\sum_{i=1}^{Ne} A_{ei} \left(\sum_{j=1}^{N} (B_{ex,t_j} - B_{ex,t_{j-1}})^2 + \sum_{j=1}^{N} (B_{ey,t_j} - B_{ey,t_{j-1}})^2 \right) \quad (18)$$

In the same way, the excess losses can be evaluated as:

$$P_{ex} = 2.p.\frac{K_e}{C_e} N.f^{1.5}.(2.N)^{0.5}.L.$$

$$\sum_{i=1}^{Ne} A_{ei} \left(\sum_{j=1}^{N} ((B_{ex,t_j} - B_{ex,t_{j-1}})^2 + (B_{ey,t_j} - B_{ey,t_{j-1}})^2)^{0.75} \right) \quad (19)$$

Concerning the second technique, a vector hysteresis model has to be adopted to describe the relation ship between magnetic flux density and magnetic field intensity in the studied machine in order to take into account the rotational magnetic field. In fact, the magnetic field in an electrical machine is not unidirectional.

In the present work, the vector Preisach model is selected to be adopted to handle the static hysteresis component for certain reasons. Indeed, it is by now considered the most employed hysteresis model. It is considered an efficient tool for hysteresis modeling since it is a phenomenological approach. Additionally, it is characterized by an elegant mathematical formalism.

According to this theory, the predicted H is given by [29]:

$$H = \frac{2}{\pi} \Delta\theta \sum_{n=1}^{N_d} H_{\theta_n}^{s-v}(B.e_{\theta_n}) e_{\theta_n} \quad (20)$$

Where

N_d is the number of direction

e_θ is the unit vector along the direction defined by the angle θ.

$H_{\theta_n}^{s-v}$ is the geometric projection of H, determined by the scalar Preisach model in the direction along e_{θ_n}.

In practice, handling the hysteresis behavior of a magnetic material using the vector Preisach model requires the determination of the Preisach density. So, the parameters of the used function have to be carefully identified in order to accurately model the hysteretic behavior. In our case, the used distribution function is a Lorentzian-modified one which is defined as follows [29]:

$$p(\alpha, \beta) = \frac{ka^2}{\left(a + (\frac{\alpha}{H_c} - b)^2 \right)\left(a + (\frac{\beta}{H_c} + b)^2 \right)} \quad (21)$$

Where H_c is the coercivity field.

$$a \in IR_+^* \quad (22)$$

$$b \in [1, \frac{H_s}{H_c}] \quad (23)$$

Where H_s is the magnetic field at saturation.

This approach is used to model the hysteresis loops and to predict iron losses too.

Concerning the third technique, an hybrid model is used to investigate dynamic hysteresis loops in the studied topology and to evaluate iron losses too. This model is represented by the following formulation [19]:

$$H(t,B) = H_h(t,B) + C_{cl}\frac{dB(t)}{dt} + C_{ex}\delta\left|\frac{dB(t)}{dt}\right|^{0.5} \quad (24)$$

Where

$H_h(t,B)$ represents the output of any suitable static hysteresis model.

C_{cl} is the eddy current loss coefficient.

The eddy current coefficient is given by the following expression:

$$C_{cl} = \frac{\sigma d^2}{12}$$

$$\delta = sign(\frac{dB(t)}{dt}) = \pm 1 \quad (25)$$

This parameter reflects the behavior of the magnetic flux density, whether increasing or decreasing.

In this study, the fist term of the model is calculated by applying the Preisach model.

Since this technique is employed for the computation of iron losses in a surface mounted permanent magnet motor, a vector model in developed to account for rotational magnetic field.

According to the advanced model and the hybrid one, the total power losses are computed using the Poynting vector theorem as:

$$P = \frac{1}{T}\int_T H\frac{dB}{dt}dt$$
$$= \frac{1}{T}\int_T (H_x\frac{dB_x}{dt} + H_y\frac{dB_y}{dt})dt \qquad (26)$$

The alternating power losses component can be computed as follows:

$$P_a = \frac{1}{T}\int_T |H|\frac{d|B|}{dt}\cos\alpha\, dt \qquad (27)$$

Where

α is the angle between B and H.

The rotational losses component can be evaluated as follows:

$$P_r = \frac{1}{T}\int_T \frac{d\theta}{dt}(H\times B)_z\, dt \qquad (28)$$

Where

θ is the angle between the magnetic flux field B and the x-axis.

In this work, the total power loss is calculated the Poynting vector theorem. In reality, the magnetic field components are determined from a two dimensional finite element analysis. Accordingly, the magnetic losses per element are calculated as follows:

$$P_e = \frac{1}{T}\int_T H\frac{dB}{dt}dt$$
$$= \frac{1}{T}\int_T |H_{e,tj}|\frac{d|B_{e,tj}|}{dt}dt\cos\alpha\, dt + \frac{1}{T}\int_T \frac{d\theta}{dt}(H_{e,tj}\times B_{e,tj})dt \qquad (29)$$

The used values are determined from the finite element analysis.

As it has been previously mentioned, the analysis is restricted to a half period. Consequently, the interval between consecutive time steps is determined as follows:

$$\Delta t = t_j - t_{j-1} = \frac{T}{2N} \qquad (30)$$

Where

t_j is the current instant

t_{j-1} is the previous instant.

The total magnetic losses can be obtained by summing losses per element over the elements number. So, the total magnetic losses are evaluated as follows:

$$P = 2.p.f.L.$$
$$\sum_{i=1}^{Ne} A_{ei}.\left(\begin{array}{l} \frac{1}{T}\int_T |H_{e,tj}|\frac{d|B_{e,tj}|}{dt}dt + \\ \frac{1}{T}\int_T \frac{d\theta}{dt}(H_{e,tj}\times B_{e,tj})_z\, dt \end{array}\right) \qquad (31)$$

4. Application to a synchronous permanent magnet motor

4.1 Machine data

The studied machine, illustrated in Fig. 1, is a 3-phase, 4-poles, 48-stator slots configuration. This topology is synchronous surface-mounted permanent magnets motor with an outer rotor, a radial air gap flux and distributed windings. The stator is constructed of laminated iron (M800-65A). The rotor core is made up of iron too. The used permanent magnets are the Neodymium-Iron-Boron (NdFeB).The different parts of the machine are defined by these models: The laminated iron is defined by the initial magnetization curve. The utilized permanent magnet is defined by the relative permeability μr, the coercive force H_c and the residual flux density B_r.

The machine characteristics are given in table 1.

Table 1
Machine characteristics

Nominal torque (N. m)	Nominal output Power (kW)	Nominal Speed (rpm)
60	9.42	1500

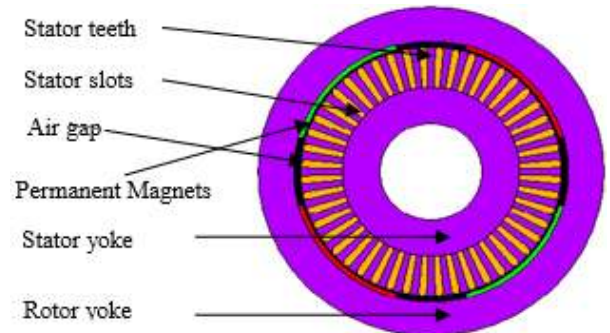

Fig. 1.General layout of the SPM [30].

The analysis of the studied machine by means of FEM is quite difficult. Due to the motor's periodicities and symmetries, we take into account one quarter of the in

the analysis process. Additionally, we apply some boundary conditions to assure the continuity of the model. The meshed study domain is illustrated in the following figure.
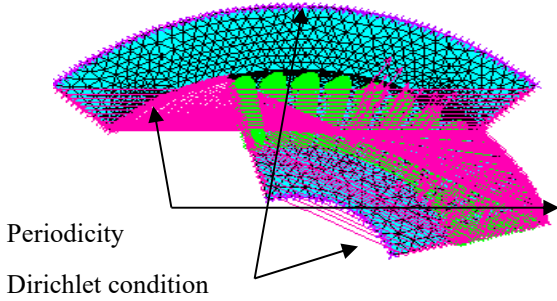

Periodicity

Dirichlet condition

Fig. 2. Meshed study domain and boundary conditions.

4.2 Finite element analysis

In this section, a two dimensional finite element analysis is carried out to investigate the magnetic field behavior in the studied machine. The two-dimensional finite-element formulation of the nonlinear problem can be expressed as follows:

$$\nabla \times \left(v_{FP} \left(\nabla \times A_z \right) \right) + \sigma \frac{\partial A_z}{\partial t} = J_z \qquad (32)$$

Where

v_{FP} is the coefficient of fixed point method.

A_z is the potential vector

J_z is the current density one.

The magnetic flux density components are determined from the above analysis results. The obtained values are then used as input of the applied models.

Primarily, the employed models have been identified using some experimental data generally provided by manufacturer. The traditional model has been identified using experimental data illustrated in the Figure 3 by minimizing the quadratic error between experimental data and calculated ones.

Similarly, the advanced model is indentified using the material technique data illustrated in Figure 5 by minimizing the quadratic error between measured data and simulated ones.
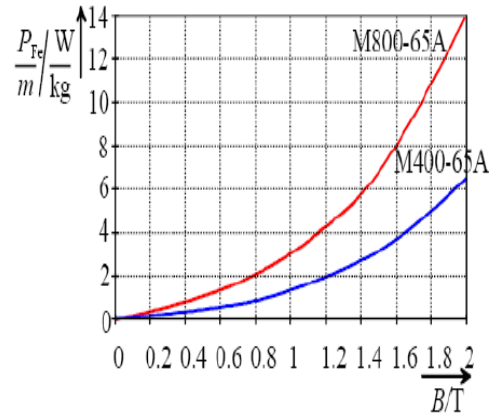

Fig.3.Experimental data of iron losses of the used material [7].

In order to prove that the Preisach model parameters are indentified properly, a comparison between the simulated and experimental major loops of the considered material is performed. The obtained result is illustrated in Fig. 5.
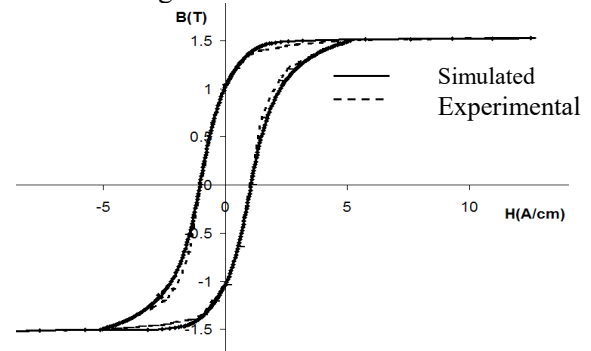

Fig.4.Experimental and simulated hysteresis loops [29].

It is clear that the obtained result is satisfactory since the modeled hysteresis loop is in a good agreement with the measured one.

Afterwards, the used models have been coupled with the two-dimensional finite-element analysis. In the case where the advanced technique and the hybrid ones are used, an iterative method ought to be employed to invert the applied models in order to be suited for modeling hysteresis phenomenon when coupled with the finite element equations. In the literature, several iterative methods have been given to deal with this problem: Fixed point technique or Newton-Rapshon method.

In this work, the fixed point technique is chosen to be employed as it is suitably stable and able to cope with nonlinearity.

5. Simulation results

After the implementation of the advanced model and the hybrid one, we investigate the static hysteresis behaviour and we determine the dynamic hysteresis

loops in such point in the machine. In fact, local computation has been carried out in particular elements belonging to a stator tooth. The obtained results are illustrated in Figs. 5, 6, 7 and 8.
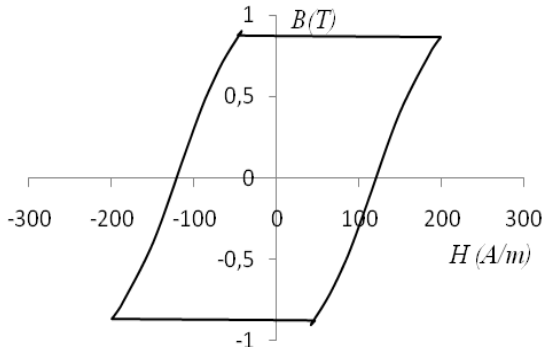

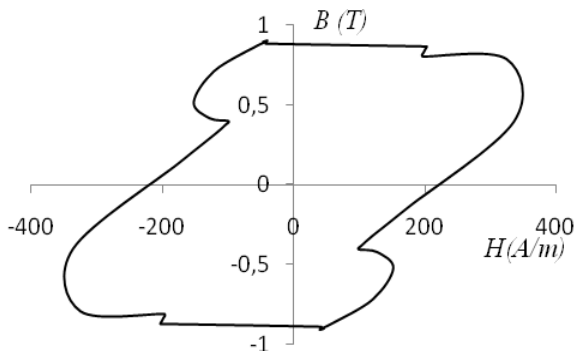Fig.5.Static hysteresis loop at a point in the middle of a tooth.

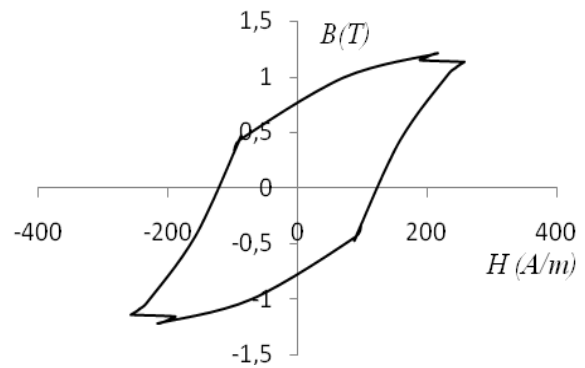Fig.6. Dynamic hysteresis loop at a point in the middle of a tooth.

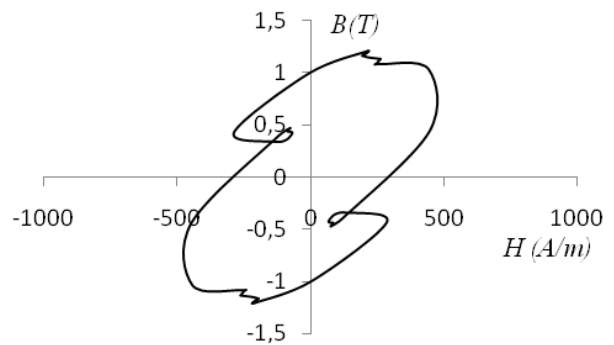Fig.7. Static hysteresis loop at a point in the root of a tooth.

Fig.8. Dynamic hysteresis loop at a point in the root of a tooth.

Referring to the previous figures, one can notices that dynamic loops are quite bigger than the static hysteresis one. This proves that the hybrid techniques, takes into account dynamic effects. Also, we can remark that both models consider minor loops. According to Figure 9, we notice that the effect of minor loops is so clear. So, we can deduce that hybrid technique is able to take small details into account. Consequently, it is clear that both hysteresis models model hysteresis loops properly. Particularly, the static hysteresis model is more comprehensible while the hybrid model is general.

After the investigation of magnetic field in the machine, iron losses are computed using models developed in the previous sections (see table 2).

Table 2
Machine iron losses under load conditions

Models	Traditional technique	Advanced technique	Hybrid technique
Total losses (W)	386.87	507.63	536.37
Hysteresis losses (W)	253.96	417.09	445.83

Accordingly to the previous table, it is obviously clear that the losses determined using the traditional method is the lowest value. This is because of the use of the lossless single-valued magnetization curve. In other words, the iron losses value does not affect the machine characteristics.

In contrary, we can remark that the value of iron losses computed using the hybrid technique is the highest value. This is due essentially the fact that hybrid technique account of small physique details. This technique is physically based so it affects the physique phenomena inside the machine.

Similarly, the value of iron losses computed using the Preisach model is comparable to the value calculated using the hybrid model. Subsequently, the obtained results are quite reasonable.

Referring to the previous table, we notice that the value of hysteresis losses predicted using the advanced technique and the hybrid one is quite higher than the one estimated using the traditional technique. This confirms the accuracy and the efficiency of the hysteresis models

since they are physically based and they affect the machine characteristics. Moreover, all the models are stable.

6. Conclusion

This work deals with the investigation of iron losses in a surface mounted permanent magnet motor. At first, a summary of general iron loss models has been presented. Indeed, these models may be classified under two groups. The first group represents models which evaluate losses by post processing the magnetic field solution. Hence, losses are not incorporated into the magnetic field solution. The second group corresponds to models that integrate losses into the magnetic field solution. Afterward, a dynamic modeling of the studied machine is performed using the finite element method. Then, three loss models have been incorporated into two dimensional stepped finite element analysis to evaluate iron losses in the studied machine. The reason of testing some different loss models is to discuss their advantages and disadvantages and to discuss their applicability, stability and efficiency as well. Finally, the obtained results are compared and analyzed. Based on the obtained results, it is shown that the post processing model is the fastest one. It is stable too. But, it is simplistic since it post processes the magnetic solution. On the contrary, the advanced model and the hybrid one requires lots of time to converge. Nevertheless, they are phenomenological. So, they influence the magnetic features of the machine. Particularly, the hybrid technique is more general, it accounts of the majority of physique phenomena and it is stable too.

References

1. Mansouri, A., Smairi, N., Trabelsi, H.: *Multi-objective optimization of an in-wheel electric vehicle motor*. In: International Journal of Applied Electromagnetics and Mechanics, 50(2016), No. 3, March 2016, p. 449-465.
2. Zhao, J., Li, B., GU, Z. : *Research on an axial flux PMSM with radially sliding permanent magnets*. In: Energies, 8(2015), No. 3, March 2015, p.1663-1684.
3. Liu, X., Du, J., Liang, D.: *Analysis and speed ripple mitigation of a space vector pulse width modulation-based permanent magnet synchronous motor with a particle swarm optimization algorithm*. In: Energies, 9(2016), No.11, November 2016, p. 923.
4. Chu, W.Q., Zhu, Z.Q., Chen, J.T.: *Simplified analytical optimization and comparison of torque densities between electrically excited and permanent-magnet machines*. In: IEEE Transactions on Industrial Electronics, 61(2014), No. 9, September 2014, p.5000-5011.
5. Mansouri, A., Msaddek, H., Trabelsi, H.: *Optimum design of a surface mounted fractional slots permanent magnet motor*. In: International Review of Electrical Engineering, 10 (2015), No. 1, February 2015, p. 28-35.
6. Mi, C., Slemon, G. R., Bonert, R.: *Modeling of iron losses of surface mounted permanent magnet synchronous motors*. In: International Proceedings of IEEE IAS 36th Annual Meeting, 4(2001), September 30-October 4, 2001, p.2585–2591, Chicago, USA.
7. Mansouri, A., Trabelsi, H., Gmiden, M. H. : *Iron losses calculation of a surface-mounted permanent magnet motor in transient finite element analysis*. In: CD-ROM 4th IEEE International Conference on Signals Systems Decision and Information Technology SSD '07, March 19-22, 2007, Tunisia, Vol. II.
8. Trabelsi, H., Mansouri, A. Gmiden, M. H. : *On the No-load iron losses calculation of a SMPM using VPM and transient finite element analysis*. In: International journal of sciences and techniques of Automatic control & computer engineering, 2(2008), No. 1, July 2008, p. 470-483, Tunisia.
9. Tian, Z. Zhang, Ch., Zhang, Sh.: *Analytical calculation of magnetic field distribution and stator iron losses for surface-mounted permanent magnet synchronous machines*. In: Energies, 10(2017), No. 3, March 2017, p. 320, Hong Kong.
10. Steinmetz, C.: *On the law of hysteresis*. In: Proceedings of the IEEE, 72(1892), No. 2, January 1892, p. 197–221.
11. Jordan, H.: *Die ferromagnetischen Konstanten für schwache Wechselfelder (Ferromagnetic constants for weak fields)*.In: Elektr. Nach. Techn, 1(1924), p. 8, Berlin.
12. Bertotti, G.: *General properties of power losses in soft ferromagnetic materials*. In: IEEE Transactions on Magnetics, 24(1988), No. 1, January 1988, p. 621-630.
13. Lavers, J., Biringer, P., Hollitscher, H. : *A simple method of estimating the minor loop hysteresis loss in thin laminations*. In: IEEE Transactions on Magnetics, 14(1978), No.5, September 1978, p. 386-388.
14. Amar, M., Kaczmarek, R.: *A general formula for prediction of iron losses under nonsinusoidal voltage waveform*. In: IEEE Transactions on Magnetics, 31(1995), No.5, September 1995, p. 2504-2509.
15. Fiorillo, F., Novikov, A.: *An improved approach to power losses in magnetic laminations under nonsinusoidal induction waveform*. In: IEEE Transactions on Magnetics, 26(1990), No. 5, September 1990, p. 2904-2910.
16. Fiorillo, F., Rietto, A. M. : *Rotational and alternating energy loss vs. magnetizing frequency in SiFe laminations*. In: Journal of magnetism and magnetic materials, 83(1990), No. 1–3, January 1990, p. 402-404.
17. Bertotti, G., Boglietti, A., Chiampi, M., Chiarabaglio, D., Fiorillo, F., Lazzari, M. : *An improved estimation of*

iron losses in rotating electrical machines. In: IEEE Transactions on Magnetics, 27(1991), No. 6, November 1991, p. 5007-5009.

18. Zhu, J. G., Ramsden: *Improved formulations for rotational core losses in rotating electrical machines.* In: IEEE Transactions on Magnetics, 34(1998), No. 4, July 1988, pp. 2234-2242.

19. Dlala, E.: *A simplified iron loss model for laminated magnetic cores.* In: IEEE Transactions on Magnetics, 44(2008), No. 11, November 2008, pp. 3169-3172.

20. Preisach, F.: *Über die magnetische Nachwirkung (Loss separation in nonoriented electrical steels).* In: Zeitschrift für physik, 94(1935), No. 5–6, May 1935, p. 277-302, Berlin.

21. Hui, S. Y. R., Zhu, J.: *Numerical modeling and simulation of hysteresis effects in magnetic cores using transmission-line modelling and the Preisach theory*: In: IEE Proceedings on Electric Power Applications, 142(1995), No. 1, January 1995, p. 57-62.

22. Jiles, D. C., Atherton, D. L.: *Theory of ferromagnetic hysteresis.* In: Journal of magnetism and magnetic materials, 61(1986), No. 1-2, September 1986, p. 48-60.

23. Philips, D., Dupre, L., Melkebeek, J.: *Comparison of Jiles and Preisach hysteresis models in magneto dynamics.* In: IEEE Transactions on Magnetics, 31(1995), No.6, November 1995, p. 3551-3553.

24. Pasquale, M., Bertotti, G., Jiles, D. C., Bi, Y.: *Application of the Preisach and Jiles-Atherton models to the simulation of hysteresis in soft magnetic alloys.* In: Journal of Applied Physiques, 85(1999), No. 8, April 1999, p. 4373-4375.

25. Mayergoyz, I.D.: *Dynamic Preisach models of hysteresis.* In: IEEE Transactions on Magnetics, 24(1988), No. 6, November 1988, p. 2925-2927.

26. Bertotti, G.: *Dynamic generalization of the scalar Preisach model of hysteresis.* In: IEEE Transactions on Magnetics, 28(1992), No. 5, September 1992, p. 2599-2601.

27. Du, R., Robertson, P.: *Dynamic Jiles-Atherton model for determining the magnetic power loss at high frequency in permanent magnet machines.* In: IEEE Transactions on Magnetics, 51(2015), No. 6, p. 1-10, June 2015.

28. Song, M., Yoon, H., Yang, H., Koh, C. S.: *A generalized Chua-Type vector hysteresis model for both the non-oriented and grain-oriented electrical steel sheets.* In: IEEE Transactions on Magnetics, 47(2011), No. 5, April 2011, p. 1146-1149.

29. Mansouri, A., Trabelsi, H.: *Incorporation of vector Preisach hysteresis model in transient finite element analysis for a SMPM.* In: International Review of Electrical Engineering, 2(2007), No. 3, June 2007, p. 448-454.

30. Mel, H., Mansouri, A., Trabelsi, H. : *On the modeling of dynamic hysteresis in a permanent magnet motor using transient finite-element analysis.* In: International Renewable Energy Congress, IREC '18, March 20-22, (2018), Tunisia.